CARBON letters

Original Articles
Carbon Letters Vol. 23, 55-62 (2017)

Dispersions of partially reduced graphene oxide in various organic solvents and polymers

Hye Min Kim[1,2], Seo Gyun Kim[1] and Heon Sang Lee[1,♠]

[1]Department of Chemical Engineering, Donga-A University, Busan 49315, Korea
[2]Sangbo Co., Ltd., Suwon 16229, Korea

Article Info
Received 10 May 2017
Accepted 24 May 2017

♠Corresponding Author
E-mail: heonlee@dau.ac.kr
Tel: +82-51-200-7724

Open Access
DOI: http://dx.doi.org/10.5714/CL.2017.23.055

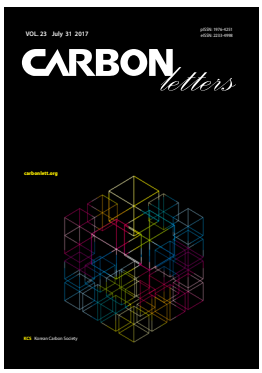

http://carbonlett.org

pISSN: 1976-4251
eISSN: 2233-4998

Abstract

We report on the dispersion state of partially reduced graphene oxide (PRGO) in organic solvents, namely methyl ethyl ketone, ethyl acetate, methylene chloride, toluene, and xylene, by controlling the carbon to oxygen (C/O) atomic ratio of the PRGOs. A two-phase solvent exchange method is also proposed to transfer PRGO from water to an aprotic solvent, such as methyl ethyl ketone. We achieve relatively good dispersion in aprotic and non-polar solvents by controlling the C/O atomic ratio of the PRGOs and applying the two-phase solvent exchange method. There is an increase in the glass transition temperatures with the dispersion of PRGOs into amorphous polymers, in particular a 4.4°C increase for poly(methyl methacrylate) and 3.0°C increase for polycarbonate. Good dispersion of PRGO in a non-polar polymer, such as linear low density polyethylene, is also obtained.

Key words: graphene oxide, organic solvent, dispersion, methyl ethyl ketone, polymers

1. Introduction

As-synthesized graphene oxide (GO) has attracted considerable attention in recent years, since the discovery of graphene [1-4]. Graphene has exceptional physical, chemical, electrical, and mechanical properties [2-4]. It has many potential applications such as polymer composites [5,6], gas barriers [7,8], transparent electrodes [9-11], gas sensors [12-14], and field effect transistors [14]. GO has four kinds of oxygen functionalities: hydroxyl (–OH), epoxide (–O–), carbonyl (–C=O), and carboxyl (–COOH) [15-17]. Epoxide and hydroxyl are located on the basal plane of GO, while carboxyl and carbonyl are located at the edge of GO [15-17]. Several groups reported the chemical reduction of GO using agents such as hydrazine [18,19], dimethylhydrazine [5], sodium borohydrazine [20], hydrogen sulfide [21], and hydroquinone [22]. Eco-friendly reduction methods have also been reported, which utilize aluminum powder [23], thermal energy [19,24,25], and ultraviolet [26].

Dispersions of GO, reduced GO (RGO), or graphene nanosheets in organic solvents are of growing research interest [26-34]. Graphene nanosheets are dispersed well in aqueous solution through electrostatic stabilization [27]. Several groups reported the exfoliation of graphite in organic solvents such as N-methyl-2-pyrrolidone (NMP) [26,28], N,N-dimethylformamide (DMF) [29,33], and o-dichlorobenzene [30]. Dubin et al. reported a solvothermal reduction method that does not use hydrazine as a reducing agent [25]. Graphene nanosheets have also been dispersed in low boiling solvents such as chloroform, isopropanol, and acetone [31]. Another study reported that as-prepared GO did not disperse in dichloromethane (methylene chloride, MC) and o-xylene [32]. GO is precipitated in a few hours and a few days, as it is dispersed in acetone, ethanol, 1-propanol, dimethyl sulfoxide (DMSO), and pyridine [32], while GO is dispersed well in ethylene glycol, DMF, NMP, and tetrahydrofuran (THF) with a long-term stability for more than 3 weeks [32]. Highly reduced graphene (HRG) is not dispersed in organic solvent if $\delta_p+\delta_h$ is less than 10 (1,2-dichlorobenzene, diethyl ether, and toluene) or much higher than 30, where δ_p and δ_h is the polarity cohesion

parameter (δ_p) and the hydrogen bonding cohesion parameter in Hansen space, respectively [33]. HRG is well dispersed in organic solvent when $\delta_p+\delta_h$ is between 10 and 30 [33].

Molecular-level dispersions of GO in polymers and biomaterials have been widely investigated [7,35-37]. In this paper, we present a new method for dispersing PRGO in good solvents for polymers such xylene for linear low density polyethylene (LLDPE), toluene for polystyrene (PS), MC for bisphenol-A polycarbonate (PC), methyl ethyl ketone (MEK) and ethyl acetate (ETA) for poly(methyl methacrylate) (PMMA), and water for poly(vinyl alcohol) (PVA). We demonstrate that PRGO is dispersed well in all the solvents studied by controlling the C/O atomic ratio and by introducing a two-phase solvent exchanging method. The methods proposed here to disperse PRGO in organic solvents and in polymers are promising for industrial applications as well as for future academic studies.

2. Experimental

2.1 Sample preparation

2.1.1. Preparation of partially reduced graphene oxide

GO was prepared from purified conventional flake graphite (19 μm nominal particle size, Asbury Carbon) by the modified Hummers method [7,38]. Chemical reduction was done with hydrazine monohydrate with stirring for 12 h at 25°C.

2.1.2. Preparation of PRGO dispersion in organic solvent

For the preparation of PRGO dispersion in MEK, the partially reduced graphene oxide (PRGO)/water solution (5 mL) was added to MEK (25 mL) and shaken for 1 min. The PRGO/water/MEK solution was centrifuged at 3000 rpm for 30 min. After centrifuging, the water and MEK was decanted leaving a PRGO band. The MEK (30 mL) was added and shaken for 1 min. After being shaken, the solution was centrifuged two times. The MEK was decanted and added, and then the PRGO/MEK solution was sonicated for 30 min. For the preparation of PRGO dispersion in ETA, the RGO/MEK solution (5 mL) was added ETA (25 mL) and shaken for 1min. The PRGO/MEK/ETA solution was centrifuged at 3000 rpm for 30 min. After centrifuging, MEK and ETA were decanted. The ETA (30 mL) was added and shaken for 1 min. After being shaken, the solution was centrifuged two times. The ETA was decanted and added, and then the PRGO/ETA solution was sonicated for 30 min. The experimental procedure to transfer PRGO from MEK to MC, toluene, and xylene was similar to that that was used for the PRGO/ETA solution.

2.1.3. Preparation of polymer/PRGO composites

To prepare the polymer/PRGO composites, we used various amorphous polymers, bisphenol-A PC ($\overline{M}_w$=30,500; TRIREX3030I, Samyang, Korea), PMMA ($\overline{M}_w$=80,778, LG DOW IH830, Korea), PS ($\overline{M}_w$=35,000, LG GPPS 15 NFI, Korea), and a semicrystalline polymer metallocene LLDPE (m-LLDPE; $\overline{M}_n$=39,000, LG, Korea). To prepare PRGO dispersion in polymers, we dissolved PMMA in MEK, PC in MC, and PS in toluene by a roll milling machine (Samheung instrument, Korea) at 100 rpm at room temperature. After that, we added the PRGO/MEK in the PMMA/MEK solution, the PRGO/MC in PC/MC solution, and the PRGO/toluene in PS/toluene solution. The PRGO/polymer/organic solvent solution was mixed by a roll milling machine at 100 rpm for 24 h. The product was dried at 40°C for 6 h and dried again in a vacuum oven at 80°C overnight. For the preparation of PRGO dispersion in m-LLDPE, m-LLDPE was dissolved in xylene by stirring at 130°C and then the PRGO/xylene solution was added to the m-LLDPE/xylene solution at 90°C. The PRGO/m-LLDPE/xylene solution was stirred for 10 min at 90°C. The product was dried at 90°C for 6 h and dried again in a vacuum oven at 80°C overnight.

2.2. Characterization

The thermal properties of polymer samples were characterized by differential scanning calorimeter (DSC) at a heating rate of 20°C/min. The glass transition temperatures and melting temperatures of the samples were measured during the second run to remove any thermal history in the fabrication process. X-ray diffraction (XRD) experiments were performed directly on the hybrid samples using a Philips (the Netherland), X'Pert-MPD system (XRD; 40 kV, 40 mA) with Cu irradiation at the scanning rate of 0.02/s in the 2 range of 2–70. Morphologies of PRGO were characterized with high-resolution transmission electron microscopy (TEM; JEM-2010, JEOL, Japan) and tapping mode atomic force microscopy (AFM). AFM images were prepared by depositing dispersions of PRGO in MEK on mica and allowing them to dry in air. TEM images were prepared by dropping the solution of PRGO in various solvents onto a 400 mesh with lacey carbon-coated copper grids and drying it under ambient conditions. X-ray photoelectron spectroscopy (XPS) was performed in a Multilab2000 with a Mg-K X-ray source using a power source of 300W. The translational diffusion coefficients were measured by a dynamic light scattering apparatus. A diode-pumped solid state laser supplied about 100 MW at λ_0=532 nm. A 256 channel digital autocorrelator was used to compute the scattered photon time autocorrelation function with a 480 ns minimum delay time. Measurements were made at several scattering angles from 30° to 90°. The polarizer had a 1:100,000 extinction ratio and the detector also had a 1:100,000 extinction ratio. The detector was rotated at a 1° resolution by a motor control unit. The electrical conductivities of the PRGO samples were measured with a Keithley 2400 electrometer, using the four-point probe technique.

3. Results and Discussion

We modified the C/O atomic ratio of PRGO by controlling the hydrazine concentration during the chemical reduction process at room temperature for 12 h. Fig. 1a shows that the C/O atomic ratio of PRGO varied with changes in the hydrazine/GO ratio during the chemical reduction process. The degree of oxidation of PRGO was investigated by XPS. The XPS spectra of as-synthesized GO and PRGO is presented in Fig. 1b and c, respectively. The peak observed at 284.1, 286.2, 288.1, 289.5 eV indicates C=C, C–O, C=O, and C=O–O, respectively. There were decreases in the contents of the oxygen functional group after the chemical reductions

as seen in Fig. 1. In this work, we counted the overall C/O atomic ratio in order to investigate the effect of the overall C/O ratio on the dispersing force of GO in organic solvents. The C/O atomic ratio of as-synthesized GO was 1.8. The C/O atomic ratios of prepared PRGOs was 3.61, 4.27, 4.47, 4.60, and 5.00, respectively. It is worth noting that the reduction of GO by hydrazine is mainly due to ring opening of the epoxides in the basal plane of GO [18,39,40]. The C/O ratios of PRGO were also estimated by measuring the electrical conductivities of PRGO coated films. The electrical conductivity of the PRGO coated films with C/O atomic ratios of 3.61, 4.27, 4.47, 4.60, and 5.00 were 163, 627, 884, 989, 1120 S/m, respectively, which is consistent with previously reported data [41].

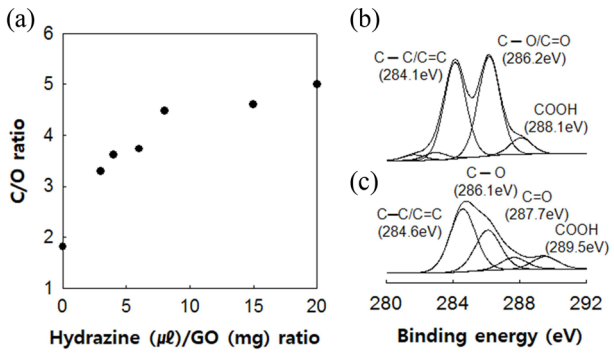

Fig. 1. Reduction of graphene oxide (GO) by hydrazine monohydrate at room temperature: (a) effect of hydrazine concentration on the C/O atomic ratio of partially reduced graphene oxide (PRGO); (b) X-ray photoelectron spectroscopy (XPS) spectra of GO (C/O ratio=1.8); (c) XPS spectra of PRGO (C/O ratio=4.6). C/O, carbon to oxygen.

We propose a two-phase solvent exchange method to transfer the PRGOs dispersed in water into MEK. MEK is one of the most widely utilized solvents in industrial processes, but it is partially miscible with water to form two phases. This method is in contrast to the single-phase solvent exchange method to disperse RGO in organic solvents such as DMF [29] and NMP [26]. Both DMF and NMP are miscible with water to form a single phase. Good dispersion of GO or RGO in various organic solvents has been reported by the single-phase solvent exchange process from NMP or DMF [42], though the high boiling points of NMP and DMF point to a disadvantage for industrial processes. Schematic illustration for two-phase solvent exchanging process is seen in Fig. 2.

When MEK is added to an aqueous GO (C/O=1.8) dispersion, two phases are observed after centrifuging. We can see that GO is located in the water phase in Fig. 2. When MEK is added to the aqueous PRGO (C/O=3.61) dispersion, two phases are also observed after centrifuging. It is striking that PRGO is located at the interface between water and MEK in Fig. 2. This may be due to the amphiphilicity of PRGO [43]. The PRGO in the band is well dispersed in MEK as seen in Fig. 2. However, the PRGO (C/O=3.61) dried at room temperature is not dispersed again in MEK as seen in Fig. 2. The interlayer spacing of dried PRGO becomes narrower after chemical reduction, and it may be difficult for MEK molecules to diffuse. The XRD pattern of natural graphite reveals a sharp reflection at 2θ=26.4°, which corresponds to the interlayer (002) spacing (d = 0.34 nm) in Fig. 3. The peak in the XRD pattern of the dried as-synthesized GO shows broadening and a shift to lower angles (2θ = 9.5°) in Fig. 3. This figure indicates that the interlayers are 0.93 nm apart

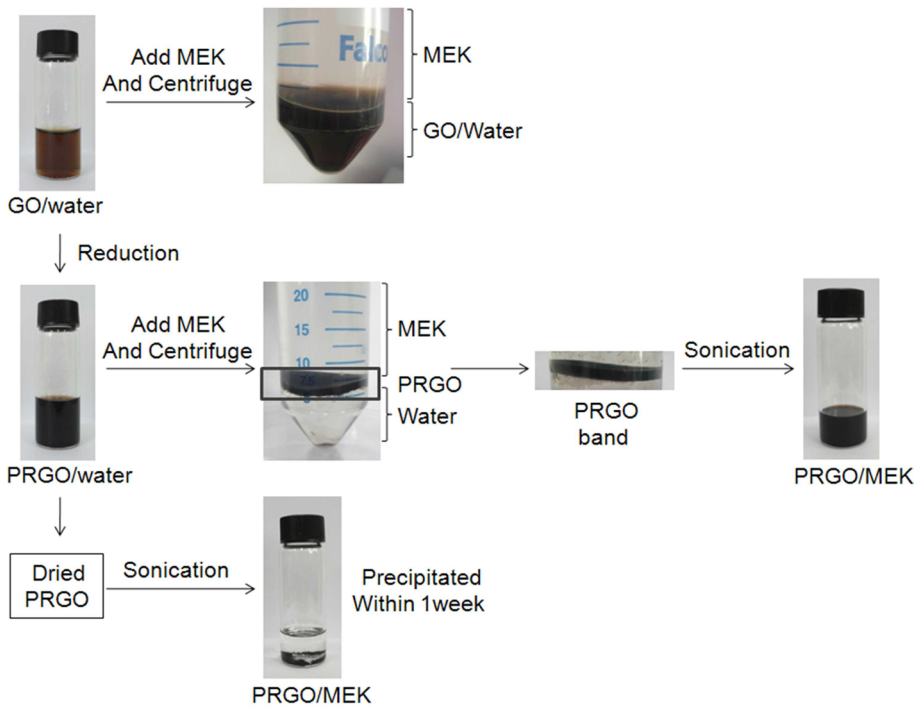

Fig. 2. Schematic illustration for the two-phase solvent exchange method. MEK, methyl ethyl ketone; GO, graphene oxide; PRGO, partially reduced graphene oxide.

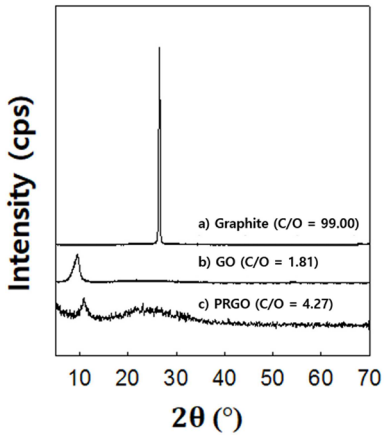

Fig. 3. X-ray diffraction patterns of graphite, graphene oxide (GO), and partially reduced graphene oxide (PRGO) with carbon to oxygen (C/O) atomic ratio 99.00, 1.81 and 4.27 respectively.

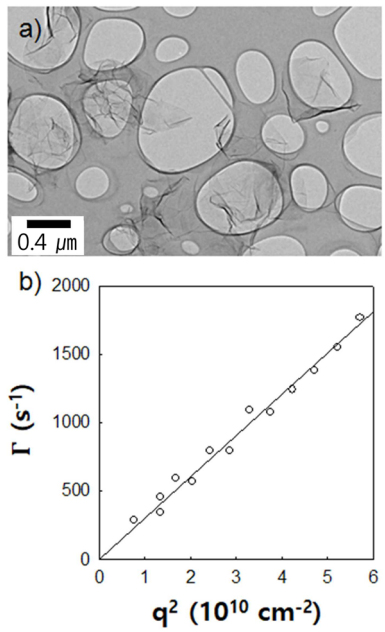

Fig. 4. Characterization of partially reduced graphene oxide dispersion in methyl ethyl ketone: (a) transmission electron microscopy image of partially reduced graphene oxide; (b) decay rates (Γ) of the electric field autocorrelation function in dynamic light scattering.

because of the intercalation by hydroxyl, carbonyl and epoxide groups and moisture. The XRD pattern of dried PRGO particles (C/O=4.27) shows a re-shift to higher angles $2\theta = 10.85^{o}$ and $2\theta = 23.2^{o}$ which correspond to interlayer spacing 0.81 and 0.38 nm.

The PRGO sheets in MEK that were characterized by TEM and dynamic light scattering are shown in Fig. 4. A TEM image of PRGO sheets suspended on a lacey carbon grid are presented in Fig. 4a and show the image of graphene with electron transparency. We employed dynamic light scattering to measure the average flake size of PRGO in a solution. The average decay rate (Γ) of the electric field autocorrelation function at 25°C is

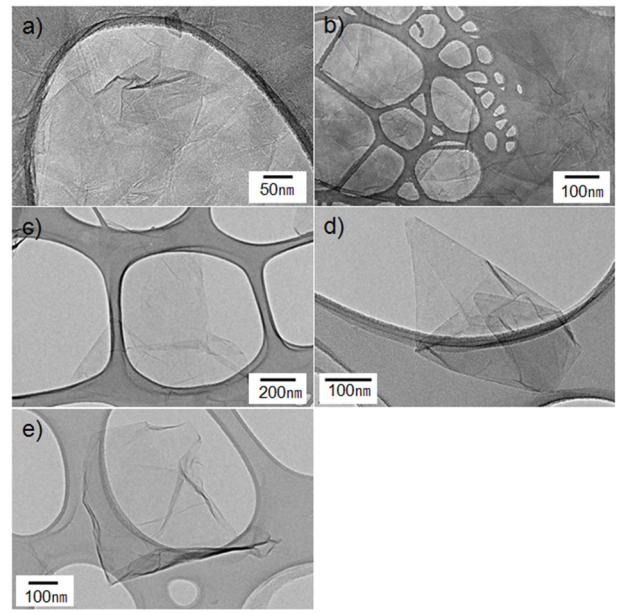

Fig. 5. Transmission electron microscopy images of partially reduced graphene oxide (PRGO) dispersed in various solvents: (a) MEK/PRGO; (b) ETA/PRGO; (c) MC/PRGO; (d) toluene/PRGO; (e) xylene/PRGO. MEK, methyl ethyl ketone; ETA, ethyl acetate; MC, methylene chloride.

shown in Fig. 4b. The first cumulant [44,45] fits the data well for all measurements. When the incident light and detector are both vertical, V_v, translational diffusion is characterized [44,46,47] by Eq. 1.

$$\Gamma_{Vv}=q^2D_T \quad (1)$$

where q is the scattering vector magnitude ($q = 4\pi n \sin(\theta/2/\lambda_0)$, n is solution refractive index, θ is the scattering angle, and λ_0 is the incident light wavelength (*in vacuo*). The translational diffusion coefficient (D_T) obtained from the slope in Fig. 4b was 3.01×10^{-8} cm^2/s. The equivalent hydrodynamic diameter of PRGO estimated by Stokes-Einstein equation ($D_H = kT/3\pi D_T\eta$) was 196 nm. The size determined by this method may be close to the weight-averaged size.

We tried to disperse various PRGOs with C/O ratios of 3.61, 4.27, 4.47, 4.60, and 5.00 into MEK. When the concentration of PRGO was lower than 0.1 mg/mL, all the RGOs were stable in MEK for more than 3 weeks, but as-synthesized GO (C/O=1.8) precipitated quickly in MEK. When the concentration of PRGO was above 0.3 mg/mL, PRGOs began to flocculate in MEK but no precipitation was observed for a week. The flocculated PRGOs were easily dispersed again in MEK by 10 min of sonication, which is confirmed by TEM images in Fig. 5. The state of dispersion can also be examined by dynamic light scattering (DLS). When the PRGO was flocculated, the average decay rate of the electric field autocorrelation function increased as seen in Fig. 6. In addition, we ascribed the scattered data in the autocorrelation function, especially at a large delay time (Fig. 6), mainly to the large flocculated particles.

We employed the single-phase solvent exchange method to transfer PRGOs from MEK to ETA, MC, toluene, and xylene,

respectively. For ETA and MC, all the PRGOs were dispersed well for 1–2 d. After 1–2 d, PRGOs began to flocculate in ETA or MC, but did not precipitate for a week. The flocculated PRGOs were easily dispersed again in ETA or MC by 10 min of sonication, which is confirmed by TEM images in Fig. 5. We changed the C/O ratio of PRGO from 3.61 to 5.00, but no appreciable difference was observed in the dispersion for ETA and MC. For toluene, the dispersion of PRGO depended on the C/O atomic ratio. When the C/O atomic ratio of PRGO was 3.61, 4.27, or 4.47, the PRGOs were precipitated in toluene within 1 min. When the C/O atomic ratio of PRGO was 4.60 or 5.00, the PRGOs were flocculated in toluene but did not precipitate for 10 h. The flocculated PRGOs were easily dispersed again in toluene by 10 min of sonication, which is confirmed by TEM images in Fig. 5. For xylene, most of the PRGOs were precipitated immediately just after sonication except for the PRGO with a C/O atomic ratio of 5.00. When the C/O atomic ratio of PRGO was 5.00, the PRGOs were flocculated in xylene but did not precipitate for 10 h. The flocculated PRGOs were easily dispersed again in xylene by 10 min of sonication, which is confirmed by TEM images in Fig. 5. The concentration of the PRGOs was higher than 0.3 mg/mL in all the studies solvents. When the concentration of the PRGOs was lower than stated above, the PRGOs were precipitated much earlier than reported above in all solvents studied except MEK.

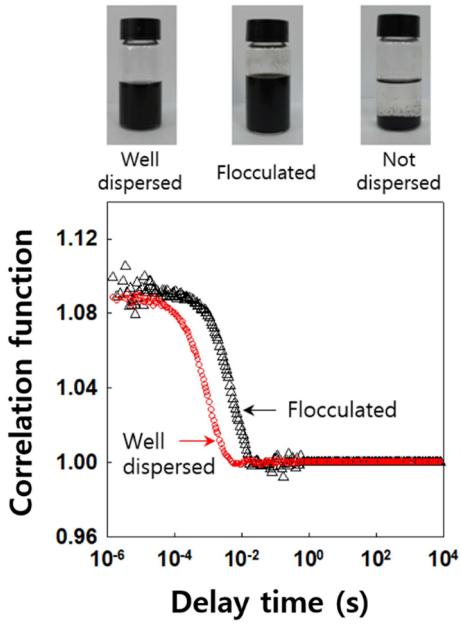

Fig. 6. Effect of the dispersion state of graphene oxide in methyl ethyl ketone on the electric field autocorrelation function.

The dispersion behaviors of PRGOs with various C/O atomic ratios in various solvents are summarized in Table 1. Good solvents for various polymers, such as LLDPE, PMMA, PS, PC, and PVA, are also listed in Table 1. We selected good solvents for polymers and PRGOs for dispersing PRGOs into a polymer from Table 1. Xylene and PRGO (C/O=5.00) were used to fabricate LLDPE/PRGO composites; toluene and PRGO (C/O=4.60) were used to fabricate PS/PRGO composites; MC and PRGO (C/O=4.47) were used to fabricate PC/PRGO composites; MEK and PRGO (C/O=3.61) were used to fabricate PMMA/PRGO composites; and water and GO (C/O=1.80) were used to fabricate PVA/GO composites. The content of PRGO in the PRGO/polymer composites was 0.7 wt% for all the studied composites. We measured the XRD patterns of polymer and polymer/PRGO nanocomposites containing 0.7 wt% to investigate the degree of exfoliation of PRGOs in various polymers. In Fig. 7, there are no PRGO characteristic peaks in the polymer/PRGO nanocomposites at $2\theta = 10.85$ and $2\theta = 23.2^{o}$. We can see only the polymer characteristic peaks. This figure indicates that the PRGO was fully exfoliated in the various polymers. We performed a thermal analysis on the PRGO/polymers composites using DSC as seen in Fig. 8. The glass transition temperatures (T_gs) of PMMA, PC and PS increased with the addition of PRGO. The increase

Table 1. The state of dispersion of RGO in various organic solvents with respect to the C/O atomic ratios relating to the Hansen solubility parameter

Polymer	Good solvents[a]	δ_P[b]	C/O atomic atios[c]					
			1.80	3.61	4.27	4.47	4.60	5.00
LLDPE	Xylene	1.0	x	x	x	x	x	△
PS	Toluene	1.4	x	x	x	x	△	△
PC	Methylene chloride	6.1	x	△	△	△	△	△
PMMA	Ethyl acetate	5.3	x	△	△	△	△	△
PMMA	Methyl ethyl ketone	9.0	x	○	○	○	○	○
PVA	Water	16.0	○	○	○	○	○	○

x : Not dispersed; the solution was precipitated immediately after sonication. △: Flocculated; the solution was flocculated but not precipitated for more than 10 h. ○: Well dispersed; at a low concentration (0.1 mg/mL), the solution was stable. At high concentration (0.3 mg/mL), the solution was flocculated but not precipitated for more than 1 wk.
RGO, reduced graphene oxide; C/O, carbon to oxygen; LLDPE, linear low density polyethylene; PS, polystyrene; PC, polycarbonate; PMMA, poly(methyl methacrylate); PVA, poly(vinyl alcohol).
[a]Good solvents used for dissolving the corresponding polymer in this work.
[b]Hansen polarity cohesion parameters of good solvents [44].
[c]Measured value of the C/O atomic ratio by X-ray photoelectron spectroscopy spectra in our laboratory.

in T_g was 4.4°C in the PMMA/PRGO composite, 3.0°C in the PC/PRGO composite, and 1.7°C in the PS/PRGO composite. The increases in T_gs of polymers with the addition of a small amount of PRGOs indicate that the molecular level dispersion of PRGOs in the polymers was achieved [48]. These results are supported by the XRD patterns as seen in Fig. 7. In particular, the increase in T_g of PMMA is more significant than those of the other polymers studied. The melting temperature of LLDPE was not affected by the addition of PRGO as seen in Fig. 8. However, the XRD result indicated that PRGO was also well exfoliated in LLDPE as seen in Fig. 7.

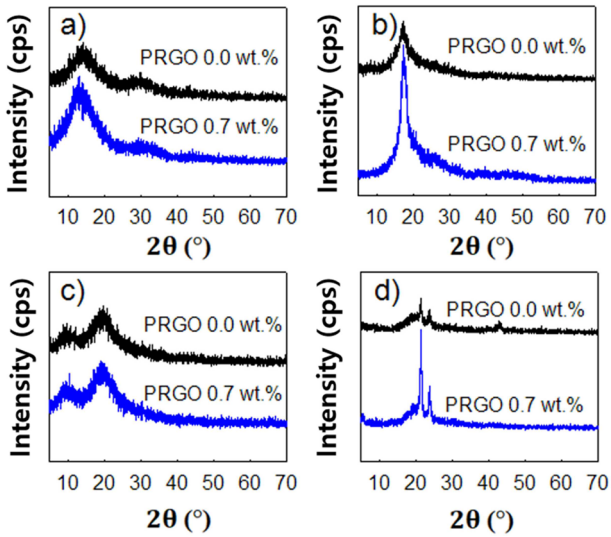

Fig. 7. X-ray diffraction patterns of polymer/partially reduced graphene oxide (PRGO) composites: (a) PMMA/PRGO; (b) PS/PRGO; (c) PC/PRGO; (d) LLDPE/PRGO. PMMA, poly(methyl methacrylate); PS, polystyrene; PC, polycarbonate; LLDPE, linear low density polyethylene.

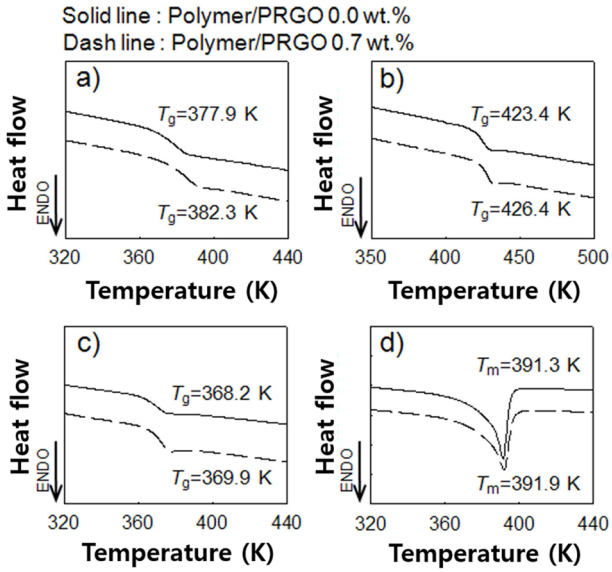

Fig. 8. Differential scanning calorimeter thermograms of polymer/partially reduced graphene oxide (PRGO) composites: (a) glass transition temperatures of PMMA in PMMA/PRGO composites; (b) glass transition temperatures of PC in PC/PRGO composites; (c) glass transition temperatures of PS in PS/PRGO composites; (d) melting temperatures of LLDPE in LLDPE/PRGO. PMMA, poly(methyl methacrylate); PC, polycarbonate; PS, polystyrene; LLDPE, linear low density polyethylene.

4. Conclusions

To summarize, the dispersion state of PRGOs in organic solvents depends on the C/O atomic ratio of the PRGOs. We proposed a two-phase solvent exchange method to transfer PRGO dispersed in water into an aprotic solvent such as MEK. Relatively good dispersion in aprotic and non-polar solvents can be obtained by controlling the C/O atomic ratio of PRGOs and applying the two-phase solvent exchange method. Molecular level dispersion of PRGO in various polymers was also obtained by using the proposed method. Appreciable increases in T_gs of amorphous polymers were observed by dispersing PRGOs in the polymers, in particular a 4.4°C increase for PMMA and 3.0°C increase for PC. We also obtained dispersion of PRGO in a non-polar polymer such as LLDPE in this study.

Conflict of Interest

No potential conflict of interest relevant to this article was reported.

Acknowledgements

This research was supported in part by the research fund from Dong-A University and in part by the Nano-Material Technology Development Program through the National Research Foundation of Korea (NRF) funded by the Ministry of Science, ICT and Future Planning (2016M3A7B4027796).

References

[1] Brodie BC. On the atomic weight of graphite. Phil Trans R Soc Lond, **149**, 249 (1859). https://doi.org/10.1098/rstl.1859.0013.
[2] Geim AK. Graphene: status and prospects. Science, **324**, 1530 (2009). https://doi.org/10.1126/science.1158877.
[3] Geim AK, Novoselov KS. The rise of graphene. Nat Mater, **6**, 183 (2007). https://doi.org/10.1038/nmat1849.
[4] Dikin DA, Stankovich S, Zimney EJ, Piner RD, Dommett GHB, Evmenenko G, Nguyen ST, Ruoff RS. Preparation and characterization of graphene oxide paper. Nature, **448**, 457 (2007). https://doi.org/10.1038/nature06016.
[5] Kim H, Abdala AA, Macosko CW. Graphene/polymer nanocomposites. Macromolecules, **43**, 6515 (2010). https://doi.org/10.1021/ma100572e.
[6] Kim M, Kim Y, Baeck SH, Shim SE. Effect of surface treatment of graphene nanoplatelets for improvement of thermal and electrical properties of epoxy composites. Carbon Lett, **16**, 34 (2015). https://doi.org/10.5714/cl.2015.16.1.034.
[7] Kim HM, Lee JK, Lee HS. Transparent and high gas barrier films based on poly(vinyl alcohol)/graphene oxide composites.

Thin Solid Films, **519**, 7766 (2011). https://doi.org/10.1016/j.tsf.2011.06.016.

[8] Bunch JS, Verbridge SS, Alden JS, van der Zande AM, Parpia JM, Craighead HG, McEuen PL. Impermeable atomic membranes from graphene sheets. Nano Lett, **8**, 2458 (2008). https://doi.org/10.1021/nl801457b.

[9] Novoselov KS, Geim AK, Morozov SV, Jiang D, Zhang Y, Dubonos SV, Grigorieva IV, Firsov AA. Electric field effect in atomically thin carbon films. Science, **306**, 666 (2004). https://doi.org/10.1126/science.1102896.

[10] Wang X, Zhi L, Müllen K. Transparent, conductive graphene electrodes for dye-sensitized solar cells. Nano Lett, **8**, 323 (2008). https://doi.org/10.1021/nl072838r.

[11] Kim KS, Zhao Y, Jang H, Lee SY, Kim JM, Kim KS, Ann JH, Kim P, Choi JY, Hong BH. Large-scale pattern growth of graphene films for stretchable transparent electrodes. Nature, **457**, 706 (2009). https://doi.org/10.1038/nature07719.

[12] Schedin F, Geim AK, Morozov SV, Hill EW, Blake P, Katsnelson MI, Novoselov KS. Detection of individual gas molecules adsorbed on graphene. Nat Mater, **6**, 652 (2007). https://doi.org/10.1038/nmat1967.

[13] Robinson JT, Perkins FK, Snow ES, Wei Z, Sheehan PE. Reduced graphene oxide molecular sensors. Nano Lett, **8**, 3137 (2008). https://doi.org/10.1021/nl8013007.

[14] Choi W, Lahiri I, Seelaboyina R, Kang YS. Synthesis of graphene and its applications: a review. Crit Rev Solid State Mater Sci, **35**, 52 (2010). http://doi.org/10.1080/10408430903505036.

[15] He H, Klinowski J, Forster M, Lerf A. A new structural model for graphite oxide. Chem Phys Lett, **287**, 53 (1998). https://doi.org/10.1016/S0009-2614(98)00144-4.

[16] Boukhvalov DW, Katsnelson MI. Modeling of graphite oxide. J Am Chem Soc, **130**, 10697 (2008). https://doi.org/10.1021/ja8021686.

[17] Cai W, Piner RD, Stadermann FJ, Park S, Shaibat MA, Ishii Y, Yang D, Velamakanni A, An SJ, Stoller M, An J, Chen D, Ruoff RS. Synthesis and solid-state NMR structural characterization of ^{13}C-labeled graphite oxide. Science, **321**, 1815 (2008). https://doi.org/10.1126/science.1162369.

[18] Lee BS, Lee Y, Hwang JY, Choi YC. Structural properties of reduced graphene oxides prepared using various reducing agents. Carbon Lett, **16**, 255 (2015). https://doi.org/10.5714/CL.2015.16.4.255.

[19] Gao X, Jang J, Nagase S. Hydrazine and thermal reduction of graphene oxide: reaction mechanisms, product structures, and reaction design. J Phys Chem C, **114**, 832 (2010). https://doi.org/10.1021/jp909284g.

[20] Si Y, Samulski ET. Synthesis of water soluble graphene. Nano Lett, **8**, 1679 (2008). https://doi.org/10.1021/nl080604h.

[21] Hofmann U, Frenzel A. Die Reduktion von Graphitoxyd mit Schwefelwasserstoff. Kolloid-Zeitschrift, **68**, 149 (1934). https://doi.org/10.1007/BF01451376.

[22] Wang G, Yang J, Park J, Gou X, Wang B, Liu H, Yao J. Facile synthesis and characterization of graphene nanosheets. J Phys Chem C, **112**, 8192 (2008). https://doi.org/10.1021/jp710931h.

[23] Fan Z, Wang K, Wei T, Yan J, Song L, Shao B. An environmentally friendly and efficient route for the reduction of graphene oxide by aluminum powder. Carbon, **48**, 1686 (2010). https://doi.org/10.1016/j.carbon.2009.12.063.

[24] McAllister MJ, Li JL, Adamson DH, Schniepp HC, Abdala AA, Liu J, Herrera-Alonso M, Milius DL, Car R, Prud'homme RK, Aksay IA. Single sheet functionalized graphene by oxidation and thermal expansion of graphite. Chem Mater, **19**, 4396 (2007). https://doi.org/10.1021/cm0630800.

[25] Dubin S, Gilje S, Wang K, Tung VC, Cha K, Hall AS, Farrar J, Varshneya R, Yang Y, Kaner RB. A one-step, solvothermal reduction method for producing reduced graphene oxide dispersions in organic solvents. ACS Nano, **4**, 3845 (2010). https://doi.org/10.1021/nn100511a.

[26] Williams G, Seger B, Kamat PV. TiO_2-grphene nanocomposites: UV-assisted photocatalytic reduction of graphene oxide. ACS Nano, **2**, 1487 (2008). https://doi.org/10.1021/nn800251f.

[27] Li D, Müller MB, Gilje S, Kaner RB, Wallace GG. Processable aqueous dispersions of graphene nanosheets. Nat Nanotechnol, **3**, 101 (2008). https://doi.org/10.1038/nnano.2007.451.

[28] Hernandez Y, Nicolosi V, Lotya M, Blighe FM, Sun Z, De S, McGovern IT, Holland B, Byrne M, Gun'Ko YK, Boland JJ, Niraj P, Duesberg G, Krishnamurthy S, Goodhue R, Hutchison J, Scardaci V, Ferrari AC, Coleman JN. High-yield production of graphene by liquid-phase exfoliation of graphite. Nat Nanotechnol, **3**, 563 (2008). https://doi.org/10.1038/nnano.2008.215.

[29] Blake P, Brimicombe PD, Nair RR, Booth TJ, Jiang D, Schedin F, Ponomarenko LA, Morozov SV, Gleeson HF, Hill EW, Geim AK, Novoselov KS. Graphene-based liquid crystal device. Nano Lett, **8**, 1704 (2008). https://doi.org/10.1021/nl080649i.

[30] Hamilton CE, Lomeda JR, Sun Z, Tour JM, Barron AR. High-yield organic dispersion of unfunctionalized graphene. Nano Lett, **9**, 3460 (2009). https://doi.org/10.1021/nl9016623.

[31] O'Neill A, Khan U, Nirmalraj PN, Boland J, Coleman JN. Graphene dispersion and exfoliation in low boiling point solvents. J Phys Chem C, **115**, 5422 (2011). https://doi.org/10.1021/jp110942e.

[32] Paredes JI, Villar-Rodil S, Martínez-Alonso A, Tascón JMD. Graphene oxide dispersions in organic solvents. Langmuir, **24**, 10560 (2008). https://doi.org/10.1021/la801744a.

[33] Park S, An J, Jung I, Piner RD, An SJ, Li X, Velamakanni A, Ruoff RS. Colloidal suspensions of highly reduced graphene oxide in a wide variety of organic solvents. Nano Lett, **9**, 1593 (2009). https://doi.org/10.1021/nl803798y.

[34] Johnson DW, Dobson BP, Coleman KS. A manufacturing perspective on graphene dispersions. Curr Opin Colloid Interface Sci, **20**, 367 (2015). https://doi.org/10.1016/j.cocis.2015.11.004.

[35] Liang J, Huang Y, Zhang L, Wang Y, Ma Y, Guo T, Chen Y. Molecular-level dispersion of graphene into poly(vinyl alcohol) and effective reinforcement of their nanocomposites. Adv Funct Mater, **19**, 2297 (2009). https://doi.org/10.1002/adfm.200801776

[36] Yadav SK, Jung YC, Kim JH, Ko YI, Ryu HJ, Yadav MK, Kim YA, Cho JW. Mechanically robust, electrically conductive biocomposite films using antimicrobial chitosan-functionalized graphenes. Part Part Syst Charact, **30**, 721 (2013). https://doi.org/10.1002/ppsc.201300044.

[37] Noh YJ, Joh HI, Yu J, Hwang SH, Lee S, Lee CH, Kim SY, Youn JR. Ultra-high dispersion of graphene in polymer composite via solvent free fabrication and functionalization. Sci Rep, **5**, 9141 (2015). https://doi.org/10.1038/srep09141.

[38] Kovtyukhova NI, Ollivier PJ, Martin BR, Mallouk TE, Chizhik SA, Buzaneva EV, Gorchinskiy AD. Layer-by-layer assembly of ultrathin composite films from micron-sized graphite oxide sheets and polycations. Chem Mater, **11**, 771 (1999). https://doi.org/10.1021/cm981085u.

[39] Wang H, Hu YH. Effect of oxygen content on structures of graphite oxides. Ind Eng Chem Res, **50**, 6132 (2011). https://doi.org/10.1021/ie102572q.
[40] Lotya M, King PJ, Khan U, De S, Coleman JN. High-concentration, surfactant-stabilized graphene dispersions. ACS Nano, **4**, 3155 (2010). https://doi.org/10.1021/nn1005304.
[41] Kim SG, Lee SS, Lee E, Yoon J, Lee HS. Kinetics of hydrazine reduction of thin films of graphene oxide and the determination of activation energy by the measurement of electrical conductivity. RSC Adv, **5**, 102567 (2015). https://doi.org/10.1039/c5ra18446k.
[42] Zhang X, Coleman AC, Katsonis N, Browne WR, van Wees BJ, Feringa BL. Dispersion of graphene in ethanol using a simple solvent exchange method. Chem Commun, **46**, 7539 (2010). https://doi.org/10.1039/C0CC02688C.
[43] Kim J, Cote LJ, Kim F, Yuan W, Shull KR, Huang J. Graphene oxide sheets at interfaces. J Am Chem Soc, **132**, 8180 (2010). https://doi.org/10.1021/ja102777p.
[44] Lee HS, Yun CH. Translational and rotational diffusions of multi-walled carbon nanotubes with static bending. J Phys Chem C, **112**, 10653 (2008). https://doi.org/10.1021/jp803363j.
[45] Koppel DE. Analysis of macromolecular polydispersity in intensity correlation spectroscopy: the method of cumulants. J Chem Phys, **57**, 4814 (1972). https://doi.org/10.1063/1.1678153.
[46] Berne B, Pecora R. Dynamic Light Scattering, Wiley, New York, 114 (1976).
[47] Cush R, Russo PS, Kucukyavuz Z, Bu Z, Neau D, Shih D, Kucukyavuz S, Ricks H. Rotational and translational diffusion of a rodlike virus in random coil polymer solutions. Macromolecules, **30**, 4920 (1997). https://doi.org/10.1021/ma970032f.
[48] Hansen CM. Hansen Solubility Parameters: A User's Handbook, Taylor & Francis, Boca Raton, 1 (2007).